A genetically encoded fluorescent reporter of ATP:ADP ratio

Jim Berg[1,2], Yin Pun Hung[1] & Gary Yellen[1]

We constructed a fluorescent sensor of adenylate nucleotides by combining a circularly permuted variant of GFP with a bacterial regulatory protein, GlnK1, from *Methanococcus jannaschii*. The sensor's affinity for Mg-ATP was <100 nM, as seen for other members of the bacterial PII regulator family, a surprisingly high affinity given that normal intracellular ATP concentration is in the millimolar range. ADP bound the same site of the sensor as Mg-ATP, competing with it, but produced a smaller change in fluorescence. At physiological ATP and ADP concentrations, the binding site is saturated, but competition between the two substrates causes the sensor to behave as a nearly ideal reporter of the ATP:ADP concentration ratio. This principle for sensing the ratio of two analytes by competition at a high-affinity site probably underlies the normal functioning of PII regulatory proteins. The engineered sensor, Perceval, can be used to monitor the ATP:ADP ratio during live-cell imaging.

ATP is the primary energy currency in living cells. It also acts as a signaling molecule to coordinate responses to energy status, in part by modulating ion channels[1] and activating signaling cascades[2]. The production and consumption of ATP have been suggested in some cases to be spatially restricted (or 'compartmentalized') in cells[3,4]. To understand fully how such compartmentation of ATP may influence cellular physiology, a visible reporter for cellular ATP is needed. Luciferase, an ATP-consuming enzyme that produces a luminescent product[5], has been used for this purpose: it is genetically expressed in cells, the substrate luciferin is applied, and the resultant ATP-dependent luminescence can be imaged with a photon-counting charge coupled device (CCD) camera[6,7], but general use of this approach is limited by very low signal levels. A fluorescent sensor of ATP would in principle allow better temporal and spatial detection of physiological changes.

Genetically encoded fluorescent biosensors have been created from GFP and its variants using various strategies. Some of these use circularly permuted fluorescent proteins (cpFPs), in which the original N and C termini are connected via a peptide linker, and new N and C termini are created in close proximity to the chromophore[8]. The calcium sensor pericam[9] and hydrogen peroxide sensor HyPer[10] have been created by fusing the N and C termini of a cpFP to specific detector proteins for calcium or hydrogen peroxide, respectively. Conformational changes in the fusion proteins caused by the binding of the analyte to the detector protein domain lead to changes in sensor fluorescence.

We sought a suitable ATP-binding protein with which to use this cpFP approach. The ATP-binding bacterial protein GlnK1, a member of the PII family, is a trimeric intracellular protein that regulates ammonia transport associated with the synthesis of glutamine. In its apo (unliganded) form, it binds to a bacterial ammonia transporter and blocks ammonia import. Only when the GlnK1 protein has bound both Mg-ATP and 2-ketoglutarate, indicating a healthy metabolism and glutamine synthesis precursor availability, does it dissociate from the transporter and permit ammonia transport into the bacterium[11–13]. Binding of Mg-ATP to GlnK1 results in a dramatic conformational change[13] in which the 'T loop' (Gly37–Val53) changes from a very loose disordered structure to a compact ordered loop (**Fig. 1a**). Because of this localized structural change upon ATP binding, we used GlnK1 as a backbone for a fluorescent ATP sensor.

We used the cpFP approach to create an improved cellular ATP biosensor based on GlnK1. Integration of a yellow cpFP, circularly permuted monomeric Venus (cpmVenus), into the T loop of GlnK1 yielded a fluorescent sensor of ATP. We found that this sensor (and likely the native GlnK1 protein) reported the ratio of ATP/ADP levels. An optimized version of this probe expressed in mammalian cells responded to inhibition of cellular metabolism with real-time changes in fluorescence.

RESULTS

A cpFP inserted into GlnK1 reports ATP with high affinity

To engineer an ATP sensor, we inserted cpmVenus into each of six sequential positions (residues Gly48 to Asp54) within the T loop of GlnK1. We expressed these fusion proteins in bacteria and assayed the purified proteins for a fluorescence response to ATP application. Most constructs were fluorescent but did not change fluorescence upon application of ATP. But in the fusion with cpmVenus inserted between Tyr51 and Ile52, a construct named QV5, there was a substantial change in the excitation spectrum upon ATP application (**Fig. 1b**). The basal excitation spectrum of this construct was similar to that of YFP, with a prominent peak around 490 nm and an additional, smaller peak at 405 nm. As ATP was

[1]Department of Neurobiology, Harvard Medical School, 220 Longwood Ave., Boston, Massachusetts 02115, USA. [2]Present address: Department of Physiology, University of California, 1550 4th Street, San Francisco, California 94158, USA. Correspondence should be addressed to G.Y. (gary_yellen@hms.harvard.edu).

RECEIVED 12 JULY 2008; ACCEPTED 17 NOVEMBER 2008; PUBLISHED ONLINE 4 JANUARY 2009; CORRECTED ONLINE 11 JANUARY 2009 (DETAILS ONLINE); DOI:10.1038/NMETH.1288

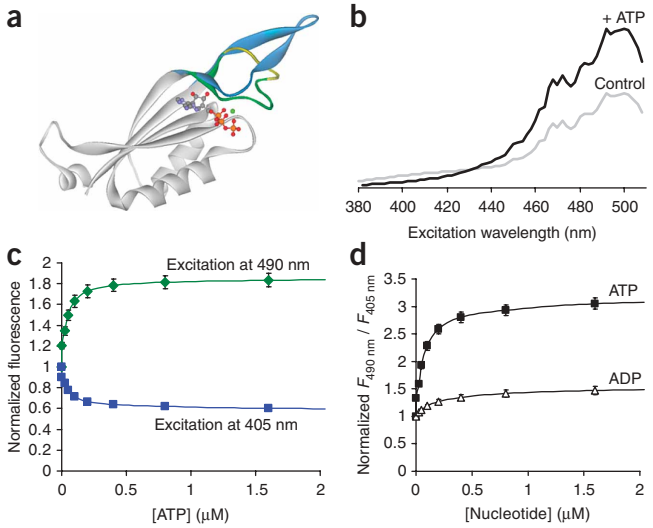

Figure 1 | Properties of the GlnK1-cpmVenus QV5 construct. (**a**) Ribbon representation of one subunit of the GlnK1 protein without a ligand (gray and blue) or with Mg^{2+}-ATP (gray, green and yellow, with the ligand in ball-and-stick form) based on Protein Data Bank files 2j9e and 2j9d (ref. 13). The blue structure is just one of the many alternative and disordered structures observed for the unliganded T loop. The yellow region indicates the insertion points used for the cpFP. (**b**) Excitation spectra of purified QV5 construct under control conditions and after addition of 50 μM Mg-ATP (emission at 530 nm). (**c**) Fluorescence intensities when exciting at 490 nm or 405 nm, normalized to the initial value; emission at 530 nm. (**d**) The ratio of fluorescence intensities when exciting at 490 nm divided by 405 nm ($F_{490\ nm}/F_{405\ nm}$) with application of ATP (affinity = ~0.04 μM) or ADP (affinity = ~0.2 μM). Error bars, ± s.e.m. ($n = 3$).

added, the 405 nm excitation peak diminished and the 490 nm peak was enhanced; thus ATP addition led to a ratiometric change in the excitation spectrum of the QV5 construct. This property, also seen for ratiometric pericam[9] and for HyPer[10], is ideal for a cellular sensor as it permits normalization of the signal irrespective of variation in the concentration of the sensor protein. As seen for the other cpFP-based probes, the shape of the emission spectrum did not change with ligand binding. Relative to cellular levels of ATP, reported to be in the millimolar range[14], the QV5 construct has a surprisingly high affinity of approximately 0.04 μM for ATP (**Fig. 1c**).

In addition to binding ATP, GlnK1 can also bind ADP, although ADP binding does not produce secure T loop closure[13]. ADP application does change the excitation spectrum of the QV5 fusion protein, although at saturating [ADP] there is only an ~1.4-fold change in the ratio of fluorescence emitted at 495 nm to that at 405 nm, compared with a roughly threefold increase with saturating [ATP] (**Fig. 1d**). The [ADP] required for a half-maximal fluorescence response was ~0.2 μM; thus, the QV5 protein has about fivefold higher affinity for ATP than for ADP.

Competition allows the sensor to report the ATP:ADP ratio

The extremely high affinity for ATP as well as the imperfect selectivity over ADP would seem to disqualify this version of the sensor for use in cellular ATP sensing, but in fact the combination of these properties leads to interesting behavior when both nucleotides are present. ATP and ADP compete for binding to the site, but only ATP causes closure of the T loop and a maximal change in fluorescence. Competition by ADP will effectively lower the affinity of the sensor for ATP. This competitive mechanism would predict that the steady-state fluorescence response of the QV5 fusion protein will depend on the ATP:ADP ratio (**Supplementary Results** online), and it will be insensitive to the absolute concentrations of the two nucleotides so long as they exceed the submicromolar affinity constants. The sensitivity should be determined by the relative affinity of the receptor for ATP and ADP. The QV5 construct has about fivefold higher affinity for ATP than for ADP, so that the sensor should be half-active when the [ATP]/[ADP] is ~0.2. We called this ratio at which the sensor response is half maximal the 'K_R' of the sensor, in analogy to the dissociation constant (K_d) of a receptor.

We tested this predicted dependence on the ATP:ADP ratio by measuring the fluorescence response to ATP application in the constant presence of different concentrations of ADP. As predicted, the response depended not on the absolute concentration of ATP alone, but rather on [ATP]/[ADP] (**Fig. 2**). When we added ATP in the presence of 5 μM ADP, the half-maximal fluorescence response occurred when [ATP] was ~1 μM (compared to ~0.04 μM when ADP was absent). This half-maximal response corresponds to an ATP:ADP ratio of ~0.2, which agrees with our expected K_R based on the ratio of ATP and ADP affinities. To test the robustness of the response, we repeated the assay with increasing concentrations of ADP (**Fig. 2**). In each case, the fluorescence response accurately reported the ATP:ADP ratio.

As for other fluorescent protein based sensors, the absolute fluorescence of the QV5 construct is sensitive to pH, but the dose-response for ATP is remarkably insensitive to pH values in the physiological range (**Supplementary Fig. 1** online). In addition, at an excitation wavelength of 435 nm the fluorescence response is isosbestic for nucleotide concentration, regardless of the pH.

The distinctive fluorescence response to ATP and ADP required Mg^{2+} (**Supplementary Results** and **Supplementary Fig. 2** online) and showed minimal interference from other ligands. Other purine nucleotides, such as AMP, NAD^+ or GTP, had little or no effect on the sensor when ADP and ATP were present (**Supplementary Fig. 3** online). We also found that application of 2-ketoglutarate, a

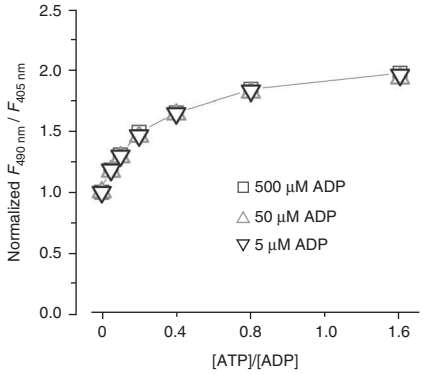

Figure 2 | The QV5 construct reports the ATP:ADP ratio. The QV5 construct fluorescence response to ATP application in the presence of 5 μM, 50 μM and 500 μM ADP showed a half-maximal response at 1 μM, 10 μM and 100 μM ATP, respectively, corresponding to a half-maximal response when [ATP]/[ADP] = ~0.2.

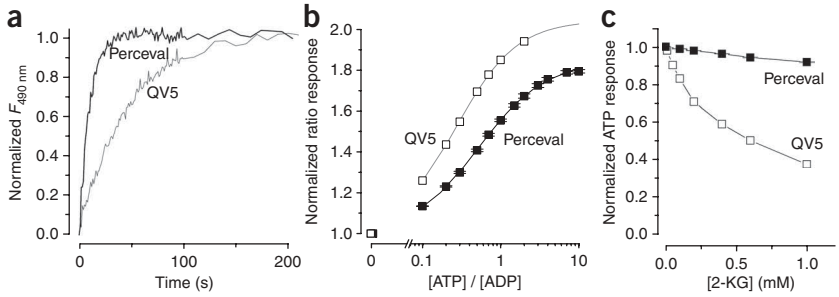

Figure 3 | Perceval is an improved version of the QV5 construct. (**a**) Kinetics of fluorescence response upon addition of a half-maximal dose of ATP to each sensor pre-equilibrated with ADP; responses were normalized to initial and final values. (**b**) Fluorescence response (495 nm/405 nm) to increasing [ATP]/[ADP], normalized to a value of 1 in the presence of saturating ADP. (**c**) Fluorescence response (495 nm/405 nm) to a saturating ATP concentration normalized to that in the absence of 2-ketoglutarate (2-KG). Error bars (± s.e.m., $n = 3$) for Perceval data are smaller than the symbols.

coactivator of the GlnK1 protein, had little effect on the basal fluorescence of the sensor. However, 2-ketoglutarate application did reduce the ATP-dependent fluorescence response in a dose-dependent manner, with an apparent affinity ($K_{apparent}$) of ~0.3 mM (**Fig. 3**).

Optimization of the ATP:ADP ratio sensor

Although the QV5 fusion protein provided a fluorescent readout of ATP:ADP ratio, it required improvement in several of its properties before we could use it as a cellular sensor. Owing to the very high affinity for both ATP and ADP, the kinetics of the response to a change in ATP:ADP ratio were quite slow, with a time constant of around a minute (**Fig. 3a**). Also, the K_R for the initial sensor, ~0.2, was likely still too low to measure interesting changes in the ATP:ADP ratio in cells, as the normal ratio in a 'fully-charged' cell[14] is in the range of 3 to 10. Lastly, the modulation by submillimolar concentrations of the intermediate metabolite 2-ketoglutarate might compromise the use of the sensor in cells.

To optimize the sensor for use in cells, we designed a semirandom mutagenesis screen on the GlnK1 portion of the sensor, targeting residues involved in the ATP binding and T loop conformational rearrangement (**Supplementary Methods** online). Using a high-throughput assay of the fluorescence response to ATP and ADP, we screened approximately 300 variants of the sensor. The best product of this screen was a sensor with improved ATP:ADP binding characteristics. This sensor contained the mutations Ala6Ser and Arg36Thr; the latter mutation affects a residue at the base of the T loop and likely alters the T loop conformational change. Then, using the product of the screen, we created a tandem trimer consisting of the modified QV5 construct linked to two modified GlnK1 protomers. The second and third protomers of this trimer have no fluorescent protein insertion and also have the T loop deleted (**Supplementary Fig. 4** online); this makes the trimer much more compact and also eliminates the opportunity for negative cooperativity reported in some native PII proteins[11]. The tandem trimer showed excellent functional expression in mammalian cells. This permuted sensor of cellular energy value, which we named Perceval, retained the spectral properties and pH and magnesium sensitivity of the original construct (**Supplementary Figs. 5** and **6** online) but had an improved K_R of ~0.5, faster kinetics and lower 2-ketoglutarate sensitivity (**Fig. 3**).

Perceval reports changes in cellular energy

To test the ability of Perceval to report changes in cellular metabolism, we expressed it in cultured HEK293 cells. The fluorescence was nearly uniform throughout the cell, and the spectral properties were very similar to those observed in the cuvette: excitation at 490 nm gave a very strong signal, whereas 430-nm excitation produced considerably lower intensities.

We used the glycolytic inhibitor 2-deoxyglucose to induce a decrease in the intracellular ATP:ADP ratio of the HEK293 cells. This inhibitor is phosphorylated by hexokinase, but it is not metabolized and acts as a competitive inhibitor of the glycolytic enzyme phosphoglucoisomerase, thus reducing cellular ATP production. Within minutes of application of 5 mM 2-deoxyglucose, we observed a sharp decrease in the fluorescence signal with 490 nm excitation. As expected from the cuvette experiments, 2-deoxyglucose induced little change in the signal when exciting at 430 nm, the isosbestic point for the ATP:ADP ratio response. The pixel-by-pixel ratio of the image taken at 490 nm divided by the 430 nm image was fairly consistent throughout the cell and this ratio decreased by ~20% upon 2-deoxyglucose application (**Fig. 4**). During this experiment, there was no change in intracellular pH, as assessed by concurrent measurements using the red pH-indicator dye SNARF-5F (Molecular Probes/Invitrogen).

Some cells showed variations in pH in response to metabolic inhibition. Because Perceval, like most other fluorescent

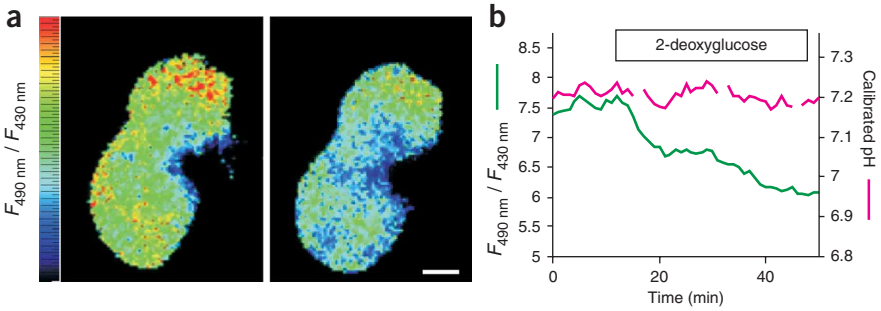

Figure 4 | Metabolic inhibition leads to a change in the Perceval signal. (**a**) A pixel-by-pixel ratio of the 490 nm excitation image by the 430 nm excitation image from two cultured HEK293 cells expressing Perceval during control conditions (left) and after 40 min of metabolic inhibition with 5 mM 2-deoxyglucose (right). Images are pseudocolored with scale of a minimum ratio of 5 (blue) and maximum of 9 (red). Scale bar, 3 μm. (**b**) Plot of $F_{490\ nm}/F_{430\ nm}$ for the bottom cell in **a** shows an ~20% decrease in the ratio after application of 5 mM 2-deoxyglucose (continuously perfused during the period indicated by the bar). Concurrent measurement of intracellular pH of the same cell with the red pH indicator dye SNARF-5F showed no change in pH.

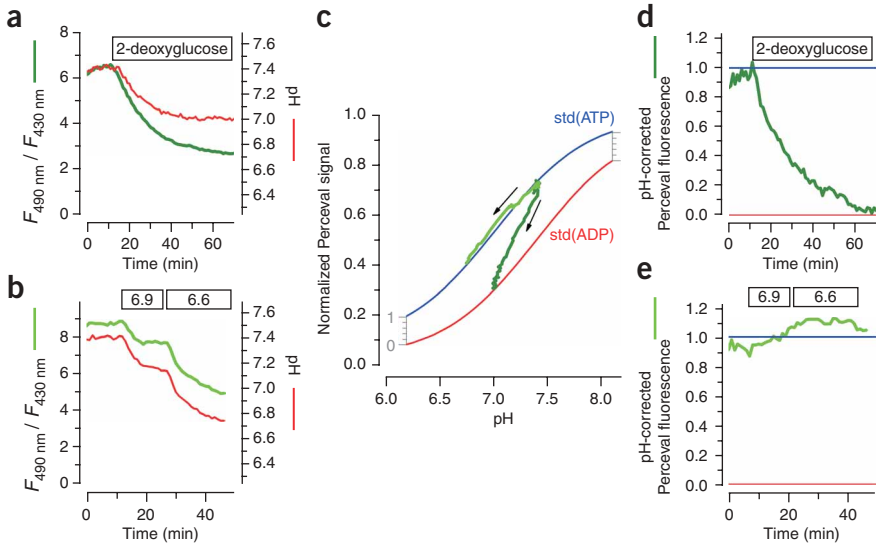

Figure 5 | Concurrent Perceval and pH monitoring, with pH correction of the Perceval signal. (**a**) Results from a cell subjected to a 2-deoxyglucose (5 mM) challenge (continuously perfused during the period indicated by the bar). pH signal was calibrated after the experiment (**Supplementary Methods**). (**b**) Results from a cell with no metabolic challenge, where the pH of the bathing solution was changed to 6.9 and then to 6.6 (as indicated by the bars). (**c**) Plot of the normalized Perceval ratio versus pH (from **a** and **b**). The two standard curves, labeled std (ATP) and std (ADP) are from cuvette assays of the ATP-loaded and ADP-loaded sensor at various pH. The initial signal was scaled to the cuvette data by assuming a starting ATP:ADP ratio of ~4. For each experiment (data from **a** are in dark green and from **b** in bright green), the arrows indicate the progression of time. Notice that pH manipulation (**b**) tracks along the pH dependence of the ATP-loaded sensor. (**d**,**e**) pH-corrected Perceval fluorescence signals from the experiments shown in **a** and **b**. The correction is done for each data point by plotting the fractional occupancy at the actual pH, as indicated by the gray scale in **c**. Blue and red lines indicated the fully ATP-and ADP-loaded states, respectively.

protein–derived sensors, is sensitive to changes in pH, we devised a strategy to isolate any fluorescence changes owing to changes in the ATP:ADP ratio from any pH-induced changes in fluorescence. By concurrently measuring intracellular pH with the pH indicator dye SNARF-5F, we could correct for any changes in the Perceval fluorescence owing to pH. We calibrated the pH measurements at the end of each experiment using various buffered solutions containing high [K^+] and nigericin to equilibrate pH across the plasma membrane (**Supplementary Fig. 7** online). The calibrated pH measurement at each time point could be used to correct the Perceval signal according to its pH dependence in the cuvette experiments. We plotted Perceval signal from a full 2-deoxyglucose experiment (**Fig. 5**) either as a function of time (**Fig. 5a**) or as a function of the pH at each time point (**Fig. 5c**). As the experiment progressed, the pH changes and the plotted points 'moved away' from the ATP-saturated curve toward the ADP-saturated curve, indicating a decline in [ATP]/[ADP]. In contrast, during a control experiment in which we exposed a cell to a low-pH bath solution (but did not metabolically challenge the cell), the intracellular pH and the raw Perceval signal changed substantially (**Fig. 5b**), but the Perceval signal data points remained superimposed on the ATP-saturated curve (**Fig. 5c**). The pH-corrected and normalized Perceval signal (**Fig. 5d,e**) indicated a clear change in the ATP:ADP ratio upon metabolic inhibition, but little change during a pure pH challenge. The pH correction appeared to be quite robust during several experiments with different pH challenges (**Supplementary Fig. 8** online).

We next tested the reversibility of the metabolic effect on the Perceval signal by transiently removing glucose from the extracellular solution. This metabolic manipulation led to a slight intracellular alkalinization and to a gradual decrease in the pH-corrected ATP:ADP ratio signal (**Fig. 6**). Upon glucose readministration, the ATP:ADP ratio signal quickly recovered to control levels.

DISCUSSION

Though we originally conceived Perceval as a sensor for ATP concentration alone, in the presence of a mixture of nucleotides, its fluorescence response was directly related not to the absolute amount of ATP, but to the ratio of ATP to ADP. This is consistent with two recent studies[15,16] that reported strong interactions between ADP and ATP on PII proteins (the class of proteins that includes GlnK1). The authors of these reports hypothesized that the competition between ATP and ADP leads these proteins to sense the 'energy charge' of the bacteria. The concept of adenylate energy charge, originally proposed in reference 17, is based on the hypothesis that although

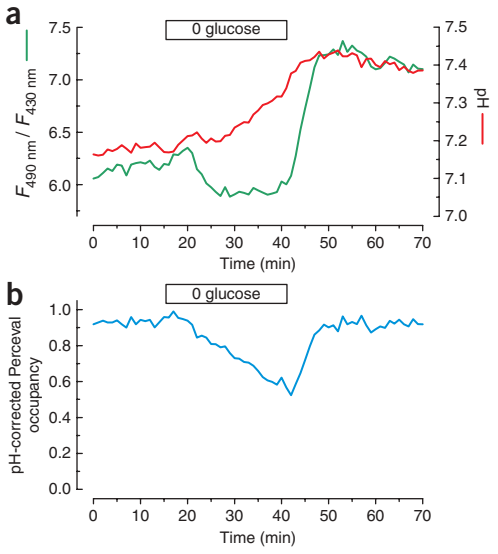

Figure 6 | Transient glucose removal leads to a reversible change in the ATP:ADP ratio signal. (**a**) A cultured HEK293 cell expressing Perceval and loaded with the pH sensitive dye SNARF-5F displayed an alkalinization when glucose was removed from the extracellular solution (10 mM glucose was replaced by equimolar sucrose). The Perceval signal showed a slight decrease upon glucose removal and a prominent rebound upon glucose addition. (**b**) The pH-corrected Perceval fluorescence signal revealed a gradual decrease in cellular energy that reversed rapidly upon glucose reapplication. Perceval occupancy of 0 corresponds to [ADP] ≫ [ATP]; occupancy of 1 corresponds to [ATP] ≫ [ADP].

the absolute individual amounts of ATP, ADP and AMP might vary widely, the ratios of ATP:ADP and ATP:AMP are more reliable indicators of metabolism from cell to cell. Detection of the cellular ATP:ADP ratio is particularly valuable because this ratio determines (along with free inorganic phosphate concentration) the actual free energy of ATP hydrolysis available for cellular reactions. Through the adenylate kinase (AdK) reaction, the ATP:ADP ratio (R) is also closely related to the free concentration of AMP, which is a critical regulator of downstream signaling mechanisms. The kinase AMPK is thought to detect the AMP:ATP ratio[18], which is approximately equal to K_{AdK}/R^2 (where K_{AdK} is the equilibrium constant for the AdK reaction).

Measurements made using tissue homogenates have demonstrated the potential for large changes in cellular ATP:ADP ratio. In mouse pancreatic beta cells, the tissue ATP:ADP ratio rises from ~2–3 to ~8–9 upon glucose stimulation[19]. The ATP:ADP ratio in rat brain tissue has been reported[14,20] as 3–8, and it has been demonstrated to fall from ~8 to ~0.4 after 2 min of ischemia[21]. Most estimates of ATP:ADP ratio are based on measurements of total nucleotide content, but the ratio of free [ATP]/[ADP] (which is detected by Perceval) is suspected to be even higher[22–24] (estimates range from twofold to 20-fold), resulting from sequestration by cellular proteins that is greater for ADP than for ATP. The effect of such ADP-binding may be substantial for cells in a high energy state, but energy depletion (below a total ATP:ADP of ~7 to 30) should rapidly saturate the ADP-binding sites (whose cellular concentration is estimated to be ~0.14 mM[23]) and produce much lower free ATP:ADP ratios, closer to the estimates for total ATP:ADP ratio.

Although the K_R of Perceval, ~0.5, is lower than most of these global measurements, the ATP:ADP ratio of single cells within tissues, and even within a single cell, is likely to vary widely because of localized energy production and consumption. The prompt depletion of energy levels we observed in HEK293 cells (with similar results in COS-7 cells; **Supplementary Fig. 9** online) indicated that Perceval can sense energy deficits, as expected in ischemia, anoxia or high energy consumption states. The present version of Perceval is better tuned for detection of energy deficits, but additional mutagenesis and selection should produce Perceval variants capable of sensing a wider range of ATP:ADP ratios.

In comparison with the existing method for measuring cellular ATP by expression of the firefly luciferase enzyme, Perceval offers many advantages. First, the light-emitting luciferase reaction depends not just on [ATP] but also on the exogenous delivery of luciferin and the presence of molecular O_2. Second, the fluorescence signal from Perceval was much stronger, so measurements can be made with brief, subsecond exposures using a traditional epifluorescence microscope and a standard CCD camera rather than the several-minute exposure using photon-counting CCDs required for luciferase detection. It should be possible to use Perceval to detect subcellular ATP localization, either by using subcellular targeting strategies as used for luciferase[7] or by optical localization using confocal, two-photon or total internal reflection fluorescence (TIRF) microscopy. Lastly, Perceval reports the energy level of the cell by competitive binding of ATP and ADP, whereas luciferase uses an ATP hydrolysis reaction that may perturb the cellular energy balance.

Approaches using nucleic acid aptamers[25,26] have recently produced sensors that distinguish ATP and ADP. This approach is promising, though the current versions have very slow kinetics and require chemical synthesis to conjugate a fluorescent dye. Also, an alternative fluorescence resonance energy transfer (FRET)–based approach to constructing a fluorescent sensor for ATP was recently described[27]. Millimolar ATP alters the FRET ratio of a tandem CFP-YFP construct, but notably, no specific ATP-binding domain is necessary for this effect. As the authors pointed out, this sounds a cautionary note for ATP interference with all FRET-based sensors. The physical basis of the effect is unclear, but it might be exploited for producing a nonratiometric measurement of ATP concentration.

One limitation of Perceval, along with all cpFP-based probes, is that its signal is sensitive to intracellular pH. Unfortunately, many metabolic perturbations also modify intracellular pH, so this sensitivity cannot easily be ignored. Glycolytic inhibition via 2-deoxyglucose has been shown to acidify the cell by ~0.2 pH units in cultured A-431 cells[28] and isolated epithelial cells[29]. We also measured acidification or alkalinization depending on the extent of metabolic inhibition of HEK 293 cells. To correct for pH effects on the Perceval signal, we measured changes in intracellular pH using the pH indicator dye SNARF-5F. Because SNARF-5F fluoresces in the red area of the spectrum, this dye can potentially also be used to correct for any pH influence on the cpFP-based probes pericam or HyPer. Conjugation of these fluorescent sensors to a pH-sensitive red protein, so that both probes are genetically encoded and targetable, may be an even better approach to pH correction.

As a tool for measuring cellular energetics, Perceval should open the door to a more complete understanding of cellular and subcellular variation in metabolism that may occur during normal cellular growth and signaling, during electrical signaling in excitable cells, and in many pathological situations such as cancer cell growth, ischemia and epileptic seizures.

METHODS

GlnK1 synthetic gene construction. A synthetic gene encoding the wild-type GlnK1 of *M. jannaschii* was designed with mammalian codon bias and with selected restriction sites to facilitate construction of the chimeric sensors. A *Kpn*I site at codons 45–47 and a *Bgl*II site at codons 53–55, flanking the T loop, were designed for insertion of the cpFP. An N-terminal 7His tag was added to facilitate purification.

Circularly permuted fluorescent protein. A circularly permuted and monomeric version of the GFP derivative Venus[30] was prepared. Standard PCR methods were used for mutagenesis and chimera construction. The final construct had its N terminus at Venus Tyr145 (numbering corresponds to standard GFP numbering); mutations H148D, Y203F and A206K; and a protein linker Gly-Gly-Ser-Gly-Gly between the original C terminus and N terminus.

Chimera construction. The circularly permuted monomeric Venus was inserted at the desired positions in the T loop using flanking PCR primers. The 5′ end of each primer consisted of 4 bases followed by the flanking restriction site (*Kpn*I or *Bgl*II) and then the desired sequence for the fusion protein; the 3′ end primed on the sequence encoding the N- or C-terminal end of the circularly permuted monomeric Venus coding sequence. After PCR with such a primer pair using the circularly permuted monomeric Venus coding sequence as template, the full-length

product was gel-purified, digested with *Kpn*I and *Bgl*II, gel-purified again, and ligated into the *Kpn*I and *Bgl*II sites of the synthetic gene encoding GlnK1.

Tandem trimer construction. The tandem trimer was constructed (using standard PCR methods) by linking a complete sensor monomer (the first protomer) to two GlnK1 monomers whose T loops were deleted (the second and third protomers; see **Supplementary Fig. 4**). The first linker inserted 13 residues (ASGGGSGGGGASG) between Gly108 of the first-protomer and Met1 of the B protomer. The second linker inserted 13 residues (ASGGGGGSGGASG) between Gly108 of the second protomer and Met1 of the third protomer. The T loop deletion in the second and third protomers eliminated GlnK1 residues 37–53 and replaced them with the linker Gly-Ala-Gly-Gly-Gly. The complete DNA and protein sequence of Perceval is given in **Supplementary Figure 10** online.

Additional methods. Details of random library construction, protein expression and purification, fluorometry, cellular imaging and pH control and calibration are available in **Supplementary Methods**.

Note: Supplementary information is available on the Nature Methods website.

ACKNOWLEDGMENTS

We thank T. Abramson for expert technical assistance with the molecular biology, A. Miyawaki (RIKEN Brain Science Institute) for sending the original plasmid encoding Venus, O. Yildiz and W. Kühlbrandt (Max Planck Institute of Biophysics, Frankfurt am Main) for sending the original plasmid encoding GlnK1, M. Merrick (John Innes Centre) for sending bacterial strains and members of the Yellen lab for their comments and discussion. This work was supported by research grants from the US National Institutes of Health –National Institute of Neurological Disorders and Stroke (NS029693 and NS055031) to G.Y.

AUTHOR CONTRIBUTIONS

G.Y. and J.B. designed the research; G.Y., J.B. and Y.P.H. conducted experiments and wrote the paper.

Published online at http://www.nature.com/naturemethods/
Reprints and permissions information is available online at http://npg.nature.com/reprintsandpermissions/

1. Ashcroft, F.M. & Gribble, F.M. ATP-sensitive K^+ channels and insulin secretion: their role in health and disease. *Diabetologia* **42**, 903–919 (1999).
2. Dennis, P.B. *et al.* Mammalian TOR: a homeostatic ATP sensor. *Science* **294**, 1102–1105 (2001).
3. Weiss, J.N. & Lamp, S.T. Cardiac ATP-sensitive K^+ channels. Evidence for preferential regulation by glycolysis. *J. Gen. Physiol.* **94**, 911–935 (1989).
4. Hoffman, J.F. ATP compartmentation in human erythrocytes. *Curr. Opin. Hematol.* **4**, 112–115 (1997).
5. Wilson, T. & Hastings, J.W. Bioluminescence. *Annu. Rev. Cell Dev. Biol.* **14**, 197–230 (1998).
6. Kennedy, H.J. *et al.* Glucose generates sub-plasma membrane ATP microdomains in single islet beta-cells. Potential role for strategically located mitochondria. *J. Biol. Chem.* **274**, 13281–13291 (1999).
7. Bell, C.J., Manfredi, G., Griffiths, E.J. & Rutter, G.A. Luciferase expression for ATP imaging: application to cardiac myocytes. *Methods Cell Biol.* **80**, 341–352 (2007).
8. Baird, G.S., Zacharias, D.A. & Tsien, R.Y. Circular permutation and receptor insertion within green fluorescent proteins. *Proc. Natl. Acad. Sci. USA* **96**, 11241–11246 (1999).
9. Nagai, T., Sawano, A., Park, E.S. & Miyawaki, A. Circularly permuted green fluorescent proteins engineered to sense Ca^{2+}. *Proc. Natl. Acad. Sci. USA* **98**, 3197–3202 (2001).
10. Belousov, V.V. *et al.* Genetically encoded fluorescent indicator for intracellular hydrogen peroxide. *Nat. Methods* **3**, 281–286 (2006).
11. Ninfa, A.J. & Jiang, P. PII signal transduction proteins: sensors of alpha-ketoglutarate that regulate nitrogen metabolism. *Curr. Opin. Microbiol.* **8**, 168–173 (2005).
12. Durand, A. & Merrick, M. In vitro analysis of the *Escherichia coli* AmtB-GlnK complex reveals a stoichiometric interaction and sensitivity to ATP and 2-oxoglutarate. *J. Biol. Chem.* **281**, 29558–29567 (2006).
13. Yildiz, O., Kalthoff, C., Raunser, S. & Kühlbrandt, W. Structure of GlnK1 with bound effectors indicates regulatory mechanism for ammonia uptake. *EMBO J.* **26**, 589–599 (2007).
14. Ereciñska, M. & Silver, I.A. Ions and energy in mammalian brain. *Prog. Neurobiol.* **43**, 37–71 (1994).
15. Wolfe, D.M., Zhang, Y. & Roberts, G.P. Specificity and regulation of interaction between the PII and AmtB1 proteins in Rhodospirillum rubrum. *J. Bacteriol.* **189**, 6861–6869 (2007).
16. Jiang, P. & Ninfa, A.J. *Escherichia coli* PII signal transduction protein controlling nitrogen assimilation acts as a sensor of adenylate energy charge *in vitro*. *Biochemistry* **46**, 12979–12996 (2007).
17. Atkinson, D.E. The energy charge of the adenylate pool as a regulatory parameter. Interaction with feedback modifiers. *Biochemistry* **7**, 4030–4034 (1968).
18. Hardie, D.G., Salt, I.P., Hawley, S.A. & Davies, S.P. AMP-activated protein kinase: an ultrasensitive system for monitoring cellular energy charge. *Biochem. J.* **338**, 717–722 (1999).
19. Nilsson, T., Schultz, V., Berggren, P.O., Corkey, B.E. & Tornheim, K. Temporal patterns of changes in ATP/ADP ratio, glucose 6-phosphate and cytoplasmic free Ca^{2+} in glucose-stimulated pancreatic beta-cells. *Biochem. J.* **314**, 91–94 (1996).
20. DeVivo, D.C., Leckie, M.P., Ferrendelli, J.S. & McDougal, D.B. Chronic ketosis and cerebral metabolism. *Ann. Neurol.* **3**, 331–337 (1978).
21. Folbergrová, J., Minamisawa, H., Ekholm, A. & Siesjö, B.K. Phosphorylase alpha and labile metabolites during anoxia: correlation to membrane fluxes of K^+ and Ca^{2+}. *J. Neurochem.* **55**, 1690–1696 (1990).
22. Veech, R.L., Lawson, J.W., Cornell, N.W. & Krebs, H.A. Cytosolic phosphorylation potential. *J. Biol. Chem.* **254**, 6538–6547 (1979).
23. Mörikofer-Zwez, S. & Walter, P. Binding of ADP to rat liver cytosolic proteins and its influence on the ratio of free ATP/free ADP. *Biochem. J.* **259**, 117–124 (1989).
24. Koretsky, A.P., Brosnan, M.J., Chen, L.H., Chen, J.D. & Dyke, T.V. NMR detection of creatine kinase expressed in liver of transgenic mice: determination of free ADP levels. *Proc. Natl. Acad. Sci. USA* **87**, 3112–3116 (1990).
25. Chiuman, W. & Li, Y. Simple fluorescent sensors engineered with catalytic DNA 'MgZ' based on a non-classic allosteric design. *PLoS ONE* **2**, e1224 (2007).
26. Huizenga, D.E. & Szostak, J.W.A. DNA aptamer that binds adenosine and ATP. *Biochemistry* **34**, 656–665 (1995).
27. Willemse, M., Janssen, E., de Lange, F., Wieringa, B. & Fransen, J. ATP and FRET–a cautionary note. *Nat. Biotechnol.* **25**, 170–172 (2007).
28. Kiang, J.G., McKinney, L.C. & Gallin, E.K. Heat induces intracellular acidification in human A-431 cells: role of Na(+)-H+ exchange and metabolism. *Am. J. Physiol.* **259**, C727–C737 (1990).
29. Brown, S.E., Heming, T.A., Benedict, C.R. & Bidani, A. ATP-sensitive Na(+)-H+ antiport in type II alveolar epithelial cells. *Am. J. Physiol.* **261**, C954–C963 (1991).
30. Nagai, T. *et al.* A variant of yellow fluorescent protein with fast and efficient maturation for cell-biological applications. *Nat. Biotechnol.* **20**, 87–90 (2002).